

BOUNDARY ELEMENT SOLUTION FOR HALF-PLANE PROBLEMS

J. C. F. TELLES and C. A. BREBBIA

Department of Civil Engineering, University of Southampton, Southampton, SO9 5NH, England

(Received 18 November 1980)

Abstract—The complete fundamental solution due to unit point loads within the half-plane is presented together with its application to the boundary element method. This solution procedure has proved to be highly accurate and computationally more efficient than the analogue implementation of Kelvin fundamental solution for problems concerning the half-plane.

Expressions for stresses at internal points are also presented and the application of the formulation to some classical problems is included.

1. INTRODUCTION

The boundary element method (B.E.M.) has become a well established numerical method of solution. It is based on a combination of classical integral equations with the versatility of curvilinear finite elements. The technique reduces the dimensionality of the problem by one and is specially well suited to problems extending to infinity. For half-space problems however, the solution would require defining a series of elements on the traction-free surface. The number of these elements, in principle needs to extend to infinity or in the best of cases, should be large enough to produce accurate solutions. Special elements extending to infinity have been proposed [6] to reduce such large discretization of the free-surface but they require further tests to validate their application. The more accurate and computationally more efficient technique is to use the half-space fundamental solution, which eliminates the need to define elements on the free-surface.

The fundamental solution for the half-plane has been presented by Melan in terms of stresses. The present paper extends it to displacements which are needed to apply the direct boundary element method. In addition, the present authors have corrected an error present in one of the original formulae by Melan. The expressions for stresses at internal points are also given in the Appendix. As far as the authors know, this complete formulation has never been presented previously, although it is of fundamental importance for the solution of problems concerning the half-plane.

The paper presents a series of examples to show the application and accuracy of the implementation.

2. FUNDAMENTAL SOLUTION FOR HALF-PLANE

The stress distribution due to point loads applied within the isotropic half-plane were presented by Melan [2]. The solution to the equivalent 3-d problem was given by Mindlin [3] who produced not only the stresses but also the corresponding displacements due to concentrated loads acting inside the half-space. The application of Mindlin's fundamental solution to boundary elements has been reported elsewhere [4] and the purpose of this paper is to present the complete solution of Melan's problem together with its application to the boundary element method.

In the present work, the traction-free surface of the half-plane is assumed to be represented by the axis $x_1 = 0$ as shown in Fig. 1.

It can be shown that Melan's fundamental solution can be represented by adding to the well known two-dimensional Kelvin fundamental solution [5] (here represented by $(\cdot)^k$) a complementary part $(\cdot)^c$ which is a function of the coordinates of the image of the load point with respect to the surface of the half-plane. Therefore, in order to avoid unnecessary repetition, only the complementary part of the tensors will be presented but it is always implied that the

s load point
 q field point
 s' image of s
 $|P_1| = |P_2| = 1$

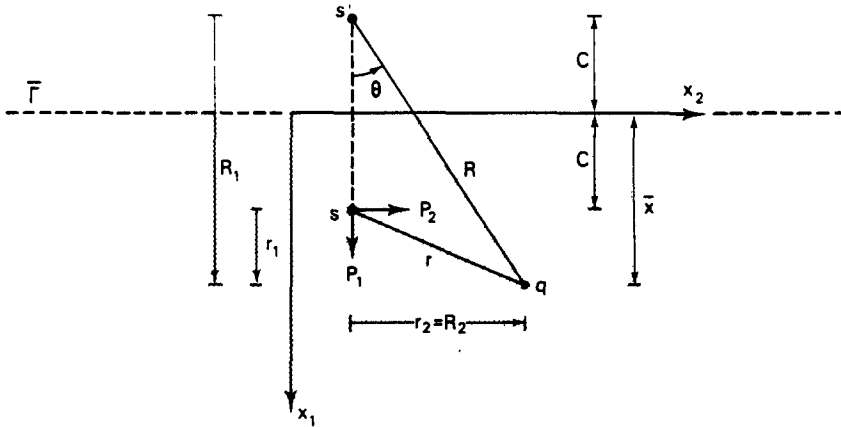


Fig. 1. Unit point loads applied within the half-plane.

total expressions of all the tensors related to the half-plane fundamental solution are given by,

$$(\)^* = (\)^k + (\)^c. \tag{1}$$

Plane strain displacements can be obtained by integrating Mindlin's expressions with reference to the out-of-plane coordinate of the load point between $-\infty$ and $+\infty$. Avoiding the tedium of algebraic operations, only the final complementary expressions for u_{ij}^c corresponding to displacements in j direction due to a unit force acting in i direction will be shown. They are as follows,

$$\begin{aligned} u_{11}^c &= K_d \left\{ -[8(1-\nu)^2 - (3-4\nu)] \ln R + \frac{[(3-4\nu)R_1^2 - 2c\bar{x}]}{R^2} + \frac{4c\bar{x}R_1^2}{R^4} \right\} \\ u_{12}^c &= K_d \left\{ \frac{(3-4\nu)r_1r_2}{R^2} + \frac{4c\bar{x}R_1r_2}{R^4} - 4(1-\nu)(1-2\nu)\theta \right\} \\ u_{21}^c &= K_d \left\{ \frac{(3-4\nu)r_1r_2}{R^2} - \frac{4c\bar{x}R_1r_2}{R^4} + 4(1-\nu)(1-2\nu)\theta \right\} \\ u_{22}^c &= K_d \left\{ -[8(1-\nu)^2 - (3-4\nu)] \ln R + \frac{[(3-4\nu)r_2^2 + 2c\bar{x}]}{R^2} - \frac{4c\bar{x}r_2^2}{R^4} \right\} \end{aligned} \tag{2}$$

where the following notation was used (see Fig. 1),

$$\begin{aligned} \theta &= \arctan(R_2/R_1) \\ r &= (r_1r_2)^{\frac{1}{2}} \\ R &= (R_1R_2)^{\frac{1}{2}} \\ r_1 &= x_i(q) - x_i(s) \\ R_1 &= x_i(q) - x_i(s') \\ c &= x_1(s) \geq 0 \\ \bar{x} &= x_1(q) \geq 0 \\ K_d &= 1/[8\pi G(1-\nu)] \\ G &: \text{shear modulus} \\ \nu &: \text{Poisson's ratio.} \end{aligned} \tag{3}$$

Stresses (σ_{jk}) corresponding to unit forces acting in i direction (here represented by σ_{jki}^*) can be taken from Melan's paper leading to the complementary expression for the traction components,

$$p_{ij}^c = \sigma_{jki}^c n_k \quad (4)$$

in which n_k stands for the direction cosines of the outward normal to the boundary of the body.

Expressions for σ_{jki}^c (plane strain) are given below; it should be noted that while checking Melan's formulae, a mistake was found and corrected in the expression for σ_{222}^c .

$$\begin{aligned} \sigma_{i11}^c &= -K_s \left\{ \frac{(3\bar{x} + c)(1 - 2\nu)}{R^2} + \frac{2R_1(R_1^2 + 2c\bar{x}) - 4\bar{x}r_2^2(1 - 2\nu)}{R^4} - \frac{16c\bar{x}R_1r_2^2}{R^6} \right\} \\ \sigma_{i21}^c &= -K_s r_2 \left\{ -\frac{(1 - 2\nu)}{R^2} + \frac{2[\bar{x}^2 - 2c\bar{x} - c^2 + 2\bar{x}R_1(1 - 2\nu)]}{R^4} + \frac{16c\bar{x}R_1^2}{R^6} \right\} \\ \sigma_{i22}^c &= -K_s \left\{ \frac{(\bar{x} + 3c)(1 - 2\nu)}{R^2} + \frac{2[R_1(r_2^2 + 2c^2) - 2cr_2^2 + 2\bar{x}r_2^2(1 - 2\nu)]}{R^4} + \frac{16c\bar{x}R_1r_2^2}{R^6} \right\} \\ \sigma_{i12}^c &= -K_s r_2 \left\{ \frac{(1 - 2\nu)}{R^2} - \frac{2[c^2 - \bar{x}^2 + 6c\bar{x} - 2\bar{x}R_1(1 - 2\nu)]}{R^4} + \frac{16c\bar{x}r_2^2}{R^6} \right\} \\ \sigma_{i22}^c &= -K_s \left\{ \frac{(3\bar{x} + c)(1 - 2\nu)}{R^2} + \frac{2[(2c\bar{x} + r_2^2)R_1 - 2\bar{x}R_1^2(1 - 2\nu)]}{R^4} - \frac{16c\bar{x}R_1r_2^2}{R^6} \right\} \\ \sigma_{i22}^c &= -K_s r_2 \left\{ \frac{3(1 - 2\nu)}{R^2} + \frac{2[r_2^2 - 4c\bar{x} - 2c^2 - 2\bar{x}R_1(1 - 2\nu)]}{R^4} + \frac{16c\bar{x}R_1^2}{R^6} \right\} \end{aligned} \quad (5)$$

where

$$K_s = 1/[4\pi(1 - \nu)]. \quad (6)$$

Expressions (2)–(6) are valid for plane stress if ν is replaced by $\bar{\nu} = \nu/(1 + \nu)$.

It is worth noting that although the complementary expressions are singular with respect to R , they do not present any singularities within the actual domain $x_1 \geq 0$ when $c > 0$ (i.e. when the load point is located inside the half-plane). For the case when the load point lies at the surface of the half-plane ($c \rightarrow 0$), it is easily seen that expressions (2)–(6), together with (1) give the displacements and tractions corresponding to Flamant's problem[7] which still produces singularities of the same order of 2d-Kelvin fundamental solution. As a consequence, the implementation of the half-plane fundamental solution to the boundary element method does not create any special difficulty and possesses the advantage of having the free-surface condition included.

3. BOUNDARY ELEMENT EQUATIONS

Different procedures for achieving the initial statement for the boundary element formulation have been presented in the literature (see[5] for references). For the half-plane implementation the same pattern can be followed leading to the equivalent starting equation

$$u_i + \int_{\Gamma} p_{ij}^* u_j d\Gamma = \int_{\Gamma} u_{ij}^* p_j d\Gamma + \int_{\Omega} u_{ij}^* b_j d\Omega \quad (7)$$

where u_j and p_j are the displacement and traction components and b_j is the body force per unit volume. The boundary of the body is represented by Γ and its interior by Ω . Note that Ω is always located within the half-plane $x_1 \geq 0$.

Equation (7), also known as Somigliana's identity, is valid for load points located inside the domain of the body.

Let us examine the boundary integral shown on the l.h.s. of (7). If the body which is being analysed presents part of its boundary coinciding with the surface of the half-plane $\bar{\Gamma}$, the integral over this part vanishes identically because of the traction-free condition included into

the fundamental solution (i.e. $p_{ij}^* = 0$ over $\bar{\Gamma}$). Consequently equation (7) can be rewritten as follows,

$$u_i + \int_{\Gamma'} p_{ij}^* u_j d\Gamma = \int_{\Gamma} u_{ij}^* p_j d\Gamma + \int_{\Omega} u_{ij}^* b_j d\Omega \quad (8)$$

where Γ' represents the part of Γ in which $x_1 > 0$.

In addition, eqn (8) can also be specialised for load points located along the surface of the half-plane $\Gamma - \Gamma'$ without any further modification. This is because when $c = 0$ the logarithmic singularity which occurs in the first integral on the r.h.s. of (8) can be integrated in the usual sense. Furthermore, if the problem to be analysed satisfies the traction-free condition ($p_j = 0$) over some part of $\Gamma - \Gamma'$, this weak singularity is also removed, allowing for load points along such part of the boundary to be considered as internal points.

As it will be seen later, the above described characteristic of the half-plane formulation plays an important role in its application to the boundary element method.

Due to the Kelvin part included into the fundamental solution, specialisation of eqn (8) for load points located along the boundary Γ' creates exactly the same singularities obtained for the single 2d-Kelvin implementation of the boundary element method. Therefore, the following equation is obtained,

$$c_{ij} u_j + \int_{\Gamma'} p_{ij}^* u_j d\Gamma = \int_{\Gamma} u_{ij}^* p_j d\Gamma + \int_{\Omega} u_{ij}^* b_j d\Omega \quad (9)$$

in which the integral on the l.h.s. is to be interpreted in Cauchy principal value sense and the expression of c_{ij} corresponds only to the Kelvin part of the fundamental solution. Hence, $c_{ij} = \delta_{ij}/2$ (δ_{ij} is the Kronecker delta) on smooth surfaces and can be taken from other references otherwise [8, 9].

The special case when the load point is located at the intersection of Γ' and $\bar{\Gamma}$ can also be handled by eqn (9). However, in this case limiting relations are used resulting in a different expression for c_{ij} . This exception does not create any difficulty and the proper expression for c_{ij} can be obtained by applying eqn (9) to represent rigid body movements.

In conclusion, eqn (9) can in general be quoted as representing the specialisation of (8) for any boundary load point if $c_{ij} = \delta_{ij}$ when referring to the boundary $\Gamma - \Gamma'$.

Following the normal boundary element procedure, the derivatives of eqn (8) with respect to the coordinates of the load point can be combined with Hooke's law to obtain the expression for internal stresses,

$$\sigma_{ij} = - \int_{\Gamma'} p_{ijk}^* u_k d\Gamma + \int_{\Gamma} u_{ijk}^* p_k d\Gamma + \int_{\Omega} u_{ijk}^* b_k d\Omega \quad (10)$$

where the complementary expressions for p_{ijk}^* and u_{ijk}^* are given in the appendix.

Note that if the problem to be analysed satisfies the traction free condition over some part of the boundary $\Gamma - \Gamma'$, stresses at boundary points along this part of the boundary can also be computed by eqn (10).

Among the different applications of the above equations, problems concerning the semi-infinite plane with or without finite cavities can be considered without requiring any outer boundary integration, provided the same regularity conditions as for Kelvin analogue implementation [1] are satisfied at infinity.

4. NUMERICAL IMPLEMENTATION

For the numerical implementation of eqn (9), the boundary is supposed to be represented by a series of elements connected to boundary nodes. These elements can be constant, linear, quadratic, etc. From the application of eqn (9) in discretized form to each boundary node, comes a series of unknowns interrelated by influence coefficients which are found by integrating over the boundary elements. For the present implementation, linear piecewise functions are chosen to interpolate displacements and tractions over the boundary elements and the body force term is not considered.

Equation (9) therefore leads to the following matrix relationship[5],

$$\mathbf{Hu} = \mathbf{Gp} \quad (11)$$

where matrix \mathbf{H} corresponds to c_{ij} plus the integral presented on the l.h.s. of (9) and similarly matrix \mathbf{G} is due to the r.h.s. integral.

Notice that the sum of c_{ij} and the corresponding principal value can be computed indirectly by imposing to (11) the condition that rigid body translations result in zero tractions. For semi-infinite medium problems it is necessary to include when considering rigid body movements the limiting value of an integral over the outer boundary,

$$\lim_{\rho \rightarrow \infty} \int_{\Gamma} p_{ij}^* d\Gamma = -\delta_{ij} \quad (12)$$

where Γ stands for the boundary of a semicircle of radius ρ within which all the cavities are contained.

For a well-posed problem, a sufficient number of tractions and boundary displacements needs to be prescribed. The unknowns are then reordered and eqn (11) takes the form,

$$\mathbf{Ax} = \mathbf{f} \quad (13)$$

where vector \mathbf{x} contains the unknown boundary displacements and tractions.

Once boundary values are known, internal values of displacements and stresses can be computed by eqns (8) and (10) in discretized form.

It is interesting to note that the use of a half-plane fundamental solution renders the discretization of the traction-free part of the boundary $x_1 = 0$ unnecessary; the displacements and stresses along this part of the surface being computed as internal points. This feature, apart from generating a smaller system of equations, avoids any numerical approximation over the free-surface. Therefore, semi-infinite or finite sized problems can be handled with equal ease.

To outline the applicability of the present formulation, some examples solved by the half-plane boundary element implementation are compared with analytical results in the next section.

5. EXAMPLES

Example 1. The first example consists of a linear traction distribution over a finite part of the boundary of the semi-infinite plane (Fig. 2). The problem was solved by discretizing the loaded part of the surface using two boundary elements only and results were computed at five internal points.

Analytical results to this problem were presented in[11] and are here compared in Tables 1 and 2. Due to the well known non-uniqueness of displacements in 2-D analysis, the vertical displacements are given with reference to the corresponding displacement of node 2.

Note that the exact agreement of the results is to be expected. Although linear interpolation functions are not exact for the boundary displacements, their contribution is removed from the analysis by the very nature of the fundamental solution.

Example 2. The next classical example is a rigid flat punch indented into the half-plane. The punch is considered to be perfectly smooth and indentation was carried out by prescribing the flat punch displacements. Boundary element analysis was performed by discretizing half of the contact surface into twelve unequally sized boundary elements. The thirteen boundary nodes were located along the discretized boundary according to the formula,

$$y = \frac{6.5(1-s)}{s}$$

where s is the node number.

Additional results were obtained at four internal points (see Fig. 3a). Note that symmetry was considered by a direct condensation process which automatically integrates over reflected elements not requiring any boundary discretization of the symmetry axis.

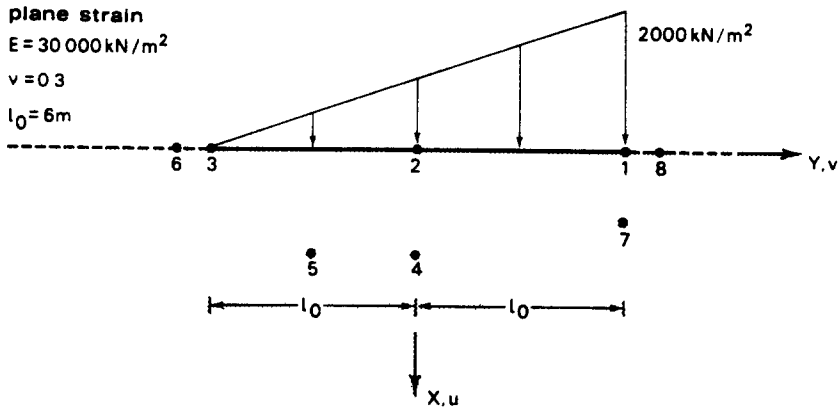


Fig. 2. Linear traction distribution problem. Boundary element discretization and internal points.

Table 1. Linear traction distribution problem. Displacements at boundary nodes

Node	$u \cdot 10^{-2}$	v	
1	-4.476	-10.400	B.E.M.
2	0.	5.200	
3	-27.649	10.400	
1	-4.476	-10.400	EXACT
2	0.	5.200	
3	-27.649	10.400	
$m \times 10^2$			

Table 2. Linear traction distribution problem. Results at internal points

Point	$u \cdot 10^{-2}$	v	σ_x	σ_y	τ_{xy}	
4	-6.251	-0.768	-959.48	-450.18	225.09	B.E.M.
5	-16.429	0.217	-514.78	-388.96	260.13	
6	-31.022	10.400	0.	0.	0.	
7	-8.394	-0.430	-894.86	-511.73	-487.48	
8	-14.719	-10.400	0.	0.	0.	
4	-6.251	-0.768	-959.48	-450.18	225.09	EXACT
5	-16.429	0.217	-514.78	-388.96	260.13	
6	-31.022	10.400	0.	0.	0.	
7	-8.394	-0.430	-894.86	-511.73	-487.48	
8	-14.719	-10.400	0.	0.	0.	
$m \times 10^2$			kN/m^2			

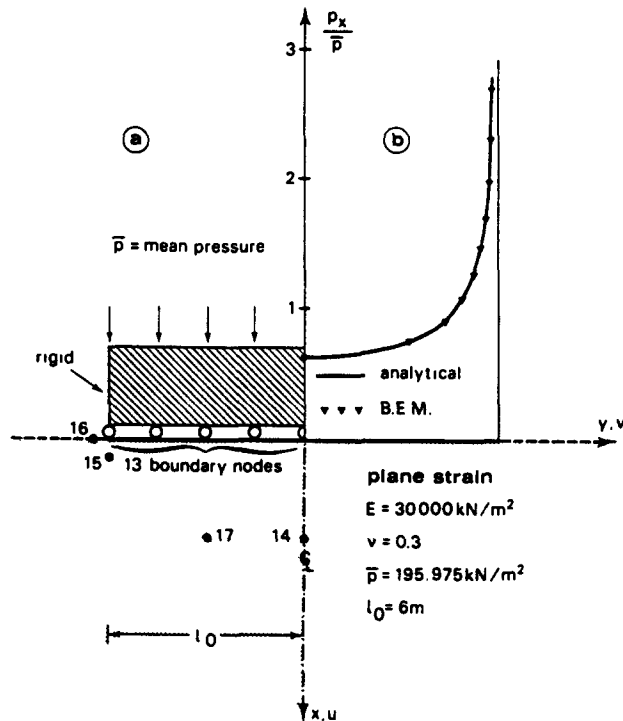


Fig. 3. Smooth punch problem: (a) problem geometry, (b) contact stresses along the discretized boundary.

Contact stresses along the discretized boundary are compared with analytical results[11] in Fig. 3(b). Apart from some traction perturbation over the tiny element connected to node thirteen, the singularity at the edge of the punch does not seem to have disturbed the results. This is also confirmed by the accuracy of the computations at internal points presented in Table 3.

Example 3. In the third application of the formulation, a semi-infinite plate with a circular hole near the straight boundary is studied. The problem is here considered under two different loading cases, unit normal pressure applied over the surface of the hole and simple tension $\bar{\sigma}_y$ parallel to the straight edge. In both cases, the stress σ_y along the traction-free straight boundary is compared with analytical results presented by Jeffery[12] and Mindlin[13] respectively.

The relatively small distance between the centre of the hole and the straight surface is 1.34 times the radius of the circle. For the boundary element analysis only the surface of the hole needs discretization and due to symmetry only half of this surface was considered.

Results for the first loading case (see Fig. 4) were computed at a series of points (considered as internal points) located along the straight boundary and 24 boundary elements of equal size were used to represent half the circle with the same area.

The second loading case was analysed by simple superposition; tractions p_y equal to the scalar product of the simple tension and the unit normal to the surface of the hole were applied to the circular boundary and the corresponding results superimposed onto the constant stress field $\bar{\sigma}_y$.

To illustrate the convergence of the method the results for 6, 12 and 24 boundary element discretizations of the half circle are compared with analytical results in Fig. 5.

It is worth mentioning that if the distance between the hole and the straight edge were larger, fewer boundary elements would be required for the same quality of results. With reference to the first loading case, for $d/r' = 1.81$, 12 boundary elements produced an error at the peak stress of about -2.7% whereas for $d/r' = 1.34$ this error was -6.5% .

6. CONCLUSIONS

The paper presents the complete formulation for the half-plane boundary element solution and shows how it can be efficiently applied to solve practical problems. It is evident that the

Table 3. Smooth punch problem. Results at internal points

Point	$u^{-1}u$	v	σ_x	σ_y	τ_{xy}	
14	-0.724	0.	-133.92	-89.28	0.	B.E.M.
15	-0.826	-1.210	-330.64	-113.16	107.93	
16	-1.824	-2.038	0.	0.	0.	
17	-0.908	-0.234	-151.87	-77.69	-3.14	
14	-0.735	0.	-133.91	-89.27	0.	EXACT
15	-0.842	-1.208	-326.47	-114.43	110.50	
16	-1.841	-2.038	0.	0.	0.	
17	-0.917	-0.234	-152.00	-77.67	-3.35	
			$m \times 10^2$		kN/m^2	

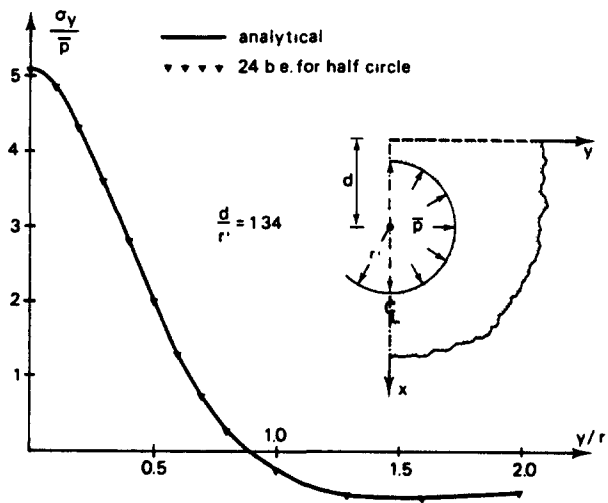


Fig. 4. Circular hole near the straight boundary under uniform pressure. Stress σ_y along the traction-free straight boundary.

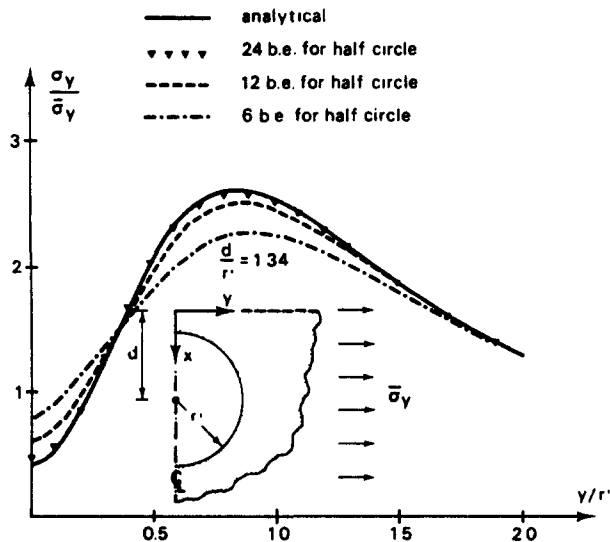


Fig. 5. Circular hole near straight boundary under remote tension parallel to the straight edge. Stress σ_y along the traction-free straight boundary.

solution procedure is much more efficient than discretizing the half-plane using finite elements or even using boundary elements with Kelvin fundamental solution, which will necessitate defining a closed boundary or using elements tending to infinity.

Application of the half-plane fundamental solution to plasticity problems following the approach presented in [10] is now under way and will be shown in a future paper.

REFERENCES

1. T. A. Cruse, *Mathematical foundations of the boundary-integral equation method in solid mechanics*. Rep. No. AFOSR-TR-77-1002, Pratt & Whitney Aircraft Group (1977).
2. E. Melan, *Der Spannungszustand der durch eine Einzelkraft in innern beanspruchten Halbscheibe*. *Z. Angew. Math. Mech.* 12, 343-346 (1932).
3. R. D. Mindlin, *Force at a point in the interior of a semi-infinite solid*. *Physics* 7, 195-202 (1936).
4. R. K. Nakaguma, *Three dimensional elastostatics using the boundary element method*. Ph.D. thesis, University of Southampton (1979).
5. C. A. Brebbia and S. Walker, *The Boundary Element Techniques in Engineering*. Butterworths, London (1979).
6. J. O. Watson, *Advanced implementation of the boundary element method for two and three-dimensional elastostatics*. In *Developments in boundary element methods I* (Edited by P. K. Banerjee and R. Butterfield), Chap. 3. Applied Science Publishers (1979).
7. A. E. H. Love, *A treatise on the mathematical theory of elasticity*. Dover, New York (1944).
8. J. C. Lachat, *A further development of the boundary integral technique for elastostatics*. Ph.D. thesis, University of Southampton (1975).
9. P. C. Riccardella, *An implementation of the boundary-integral technique for planar problems in elasticity and elasto-plasticity*. Rep. No. SM-73-10, Dept. Mech. Engineering, Carnegie-Mellon University, Pittsburg (1973).
10. J. C. F. Telles and C. A. Brebbia, *Elasto-plastic boundary element analysis*. *Proc. U.S.-Europe Workshop on Non Linear Finite Element Analysis in Structural Mechanics*, Bochum, W. Germany (July 1980).
11. H. G. Poulos and E. H. Davis, *Elastic Solutions for Soil and Rock Mechanics*. Wiley, New York (1974).
12. G. B. Jeffery, *Plane stress and plane strain in bipolar coordinates*. *Trans. R. Soc. (London)*, ser. A, 221, 265-293 (1920).
13. R. D. Mindlin, *Stress distribution around a hole near the edge of a plate under tension*. *Proc. Soc. Exptl. Stress Anal.* 5, 56-68 (1948).

APPENDIX

The complementary expressions for the tensors related to the fundamental solution are obtained by

$$u_{ik}^c = G \left(\frac{\partial u_{ik}^c}{\partial x_j} + \frac{\partial u_{jk}^c}{\partial x_i} \right) + \frac{2G\nu}{1-2\nu} \frac{\partial u_{ij}^c}{\partial x_k} \delta_{ij}$$

and

$$p_{ik}^c = G \left[\frac{\partial \sigma_{kmi}^c}{\partial x_j} + \frac{\partial \sigma_{kmi}^c}{\partial x_j} + \frac{2\nu}{1-2\nu} \frac{\partial \sigma_{kmi}^c}{\partial x_i} \delta_{ij} \right] n_m r$$

where the above derivatives are taken with reference to the coordinates of the load point. These derivatives are listed below for completeness.

$$\frac{\partial u_{11}^c}{\partial x_1} = \frac{K_d}{R^2} \left\{ [3(3-4\nu) - 8(1-\nu)^2] R_1 - 2\bar{x} + \frac{[4\bar{x}R_1 + 12c\bar{x} - 2(3-4\nu)R_1^2]}{R^2} R_1 - \frac{16c\bar{x}R_1^3}{R^4} \right\}$$

$$\frac{\partial u_{12}^c}{\partial x_1} = \frac{K_d}{R^2} r_2 \left\{ 4(1-\nu)(1-2\nu) - (3-4\nu) + \frac{[4\bar{x}(2c+\bar{x}) - 2(3-4\nu)R_1r_1]}{R^2} - \frac{16c\bar{x}R_1^2}{R^4} \right\}$$

$$\frac{\partial u_{21}^c}{\partial x_1} = \frac{K_d}{R^2} r_2 \left\{ -(3-4\nu) - 4(1-\nu)(1-2\nu) - \frac{[2(3-4\nu)R_1r_1 + 4\bar{x}(2c+\bar{x})]}{R^2} + \frac{16c\bar{x}R_1^2}{R^4} \right\}$$

$$\frac{\partial u_{22}^c}{\partial x_1} = \frac{K_d}{R^2} \left\{ 2\bar{x} - [8(1-\nu)^2 - (3-4\nu)] R_1 - \frac{[4\bar{x}r_2^2 + 2R_1((3-4\nu)r_2^2 + 2c\bar{x})]}{R^2} + \frac{16c\bar{x}R_1r_2^2}{R^4} \right\}$$

$$\frac{\partial u_{11}^c}{\partial x_2} = \frac{K_d}{R^2} r_2 \left\{ 8(1-\nu)^2 - (3-4\nu) + \frac{2[(3-4\nu)R_1^2 - 2c\bar{x}]}{R^2} + \frac{16c\bar{x}R_1^2}{R^4} \right\}$$

$$\frac{\partial u_{12}^c}{\partial x_2} = \frac{K_d}{R^2} \left\{ 4(1-\nu)(1-2\nu)R_1 + (3-4\nu)r_1 - \frac{[2(3-4\nu)R_1r_1 - 12c\bar{x}]R_1}{R^2} - \frac{16c\bar{x}R_1^3}{R^4} \right\}$$

$$\frac{\partial u_{21}^c}{\partial x_2} = \frac{K_d}{R^2} \left\{ -4(1-\nu)(1-2\nu)R_1 - (3-4\nu)r_1 + \frac{[2(3-4\nu)r_1r_2^2 + 4c\bar{x}R_1]}{R^2} - \frac{16c\bar{x}R_1r_2^2}{R^4} \right\}$$

$$\frac{\partial u_{22}^c}{\partial x_2} = \frac{K_d}{R^2} r_2 \left\{ 8(1-\nu)^2 - 3(3-4\nu) + \frac{2[(3-4\nu)r_2^2 + 6c\bar{x}]}{R^2} - \frac{16c\bar{x}r_2^2}{R^4} \right\}$$

$$\frac{\partial \sigma_{111}^c}{\partial x_1} = -\frac{K_d}{R^2} \left\{ (1-2\nu) + \frac{2[2c\bar{x} + R_1(3R_1 + 2\bar{x} - (3\bar{x} + c)(1-2\nu))]}{R^2} - \frac{8[2c\bar{x}r_2^2 + R_1(R_1(R_1^2 + 2c\bar{x}) + 4\bar{x}r_2^2\nu)]}{R^4} + \frac{96c\bar{x}R_1^2r_2^2}{R^6} \right\}$$

$$\begin{aligned} \frac{\partial \sigma_{121}^c}{\partial x_1} &= -\frac{K_1}{R^4} r_2 \left\{ 2r_1 - 4\nu(R_1 + 2\bar{x}) + 8R_1 \frac{[2\bar{x}R_1 + 6c\bar{x} - \bar{x}^2 + c^2 - 2\bar{x}R_1(1-2\nu)]}{R^2} - \frac{96c\bar{x}R_1^3}{R^4} \right\} \\ \frac{\partial \sigma_{221}^c}{\partial x_1} &= -\frac{K_1}{R^2} \left\{ 3(1-2\nu) + \frac{2[2c^2 - r_2^2 + R_1(4c - (\bar{x} + 3c)(1-2\nu))]}{R^2} + \frac{8[r_2^2(2c\bar{x} + R_1^2 - 2\bar{x}R_1(1-2\nu)) - 2c^2R_1^2]}{R^4} - \frac{96c\bar{x}R_1^2r_2^2}{R^6} \right\} \\ \frac{\partial \sigma_{111}^c}{\partial x_1} &= -\frac{K_1}{R^4} r_2 \left\{ 2(2\bar{x} - R_1)(1-2\nu) - 4(c + 3\bar{x}) + \frac{8[2\bar{x}r_2^2 + R_1(6c\bar{x} - 2\bar{x}R_1(1-2\nu) + c^2 - \bar{x}^2)]}{R^2} - \frac{96c\bar{x}R_1r_2^2}{R^4} \right\} \\ \frac{\partial \sigma_{122}^c}{\partial x_1} &= -\frac{K_1}{R^2} \left\{ (1-2\nu) + \frac{2[2c\bar{x} + r_2^2 + R_1(2\bar{x} - (7\bar{x} + c)(1-2\nu))]}{R^2} - \frac{8[2c\bar{x}r_2^2 + R_1(2\bar{x}r_2^2 + (2c\bar{x} + r_2^2)R_1 - 2\bar{x}R_1^2(1-2\nu))]}{R^4} \right. \\ &\quad \left. + \frac{96c\bar{x}R_1^2r_2^2}{R^6} \right\} \\ \frac{\partial \sigma_{222}^c}{\partial x_1} &= -\frac{K_1}{R^4} r_2 \left\{ 4\nu(3R_1 + 2\bar{x}) - 2(7R_1 + 2\bar{x}) + \frac{8R_1[4\bar{x}R_1(1-\nu) + 8c\bar{x} - r_2^2 + 2c^2]}{R^2} - \frac{96c\bar{x}R_1^3}{R^4} \right\} \\ \frac{\partial \sigma_{112}^c}{\partial x_2} &= -\frac{K_1}{R^2} r_2 \left\{ 2(7\bar{x} + c)(1-2\nu) + \frac{4[2R_1(R_1^2 + 6c\bar{x}) - 4\bar{x}r_2^2(1-2\nu)]}{R^2} - \frac{96c\bar{x}R_1r_2^2}{R^4} \right\} \\ \frac{\partial \sigma_{121}^c}{\partial x_2} &= -\frac{K_1}{R^2} \left\{ (1-2\nu) - \frac{2[\bar{x}^2 - 2c\bar{x} - c^2 + (1-2\nu)(r_2^2 + 2\bar{x}R_1)]}{R^2} + \frac{8[r_2^2(\bar{x}^2 - 2c\bar{x} - c^2 + 2\bar{x}R_1(1-2\nu)) - 2c\bar{x}R_1^2]}{R^4} + \frac{96c\bar{x}R_1^2r_2^2}{R^6} \right\} \\ \frac{\partial \sigma_{221}^c}{\partial x_2} &= -\frac{K_1}{R^4} r_2 \left\{ -2(5-6\nu)r_1 + \frac{8[R_1(r_2^2 + 2c^2 - 4c\bar{x}) - 2cr_2^2 + 2\bar{x}r_2^2(1-2\nu)]}{R^2} + \frac{96c\bar{x}R_1r_2^2}{R^4} \right\} \\ \frac{\partial \sigma_{112}^c}{\partial x_2} &= -\frac{K_1}{R^2} \left\{ -(1-2\nu) + \frac{2[(r_2^2 - 2\bar{x}R_1)(1-2\nu) + c^2 - \bar{x}^2 + 6c\bar{x}]}{R^2} - \frac{8[12c\bar{x} + c^2 - \bar{x}^2 - 2\bar{x}R_1(1-2\nu)]r_2^2}{R^4} + \frac{96c\bar{x}r_2^4}{R^6} \right\} \\ \frac{\partial \sigma_{122}^c}{\partial x_2} &= -\frac{K_1}{R^4} r_2 \left\{ 2(3\bar{x} + c)(1-2\nu) - 4R_1 + \frac{8R_1[6c\bar{x} + r_2^2 - 2\bar{x}R_1(1-2\nu)]}{R^2} - \frac{96c\bar{x}R_1r_2^2}{R^4} \right\} \\ \frac{\partial \sigma_{222}^c}{\partial x_2} &= -\frac{K_1}{R^2} \left\{ -3(1-2\nu) - \frac{2[3r_2^2 - 4c\bar{x} - 2r^2 - (2\bar{x}R_1 + 3r_2^2)(1-2\nu)]}{R^2} + \frac{8[r_2^2(r_2^2 - 4c\bar{x} - 2c^2 - 2\bar{x}R_1(1-2\nu)) - 2c\bar{x}R_1^2]}{R^4} \right. \\ &\quad \left. + \frac{96c\bar{x}R_1^2r_2^2}{R^6} \right\}. \end{aligned}$$